Royal Norwegian Council
for Scientific and Industrial Research
(NTNF)

NORSAR

NORSAR Scientific Report No. 1-88/89

Final Technical Summary

1 April – 30 September 1988

L.B. Loughran (ed.)

Kjeller, December 1988

VII.6 Comparative analysis of NORSAR and Gräfenberg Lg magnitudes for Shagan River explosions

Introduction

The seismic Lg wave propagates in the continental lithosphere and can be observed as far away as 5000 km in shield and stable platform areas (Nuttli, 1973; Baumgardt, 1985). Lg is generally considered to consist of a superposition of many higher-mode surface waves of group velocities near 3.5 km/s, and its radiation is therefore expected to be more isotropic than that of P waves. Thus, full azimuthal coverage is not essential for reliable determination of Lg magnitude. Furthermore, Lg is not affected by lateral heterogeneities in the upper mantle, which can produce strong focussing/defocussing effects of P-waves, and therefore contribute to a significant uncertainty in P-based m_b estimates.

Nuttli (1986a) showed that the amplitudes of Lg near 1 second period provide a stable estimate of magnitude, m_b(Lg) and explosion yield for Nevada Test Site explosions. He also applied his measurement methods to Semipalatinsk explosions (Nuttli, 1986b), using available WWSSN records to estimate m_b(Lg) and yields of these events.

Ringdal (1983) first suggested a method to determine Lg magnitudes based on digitally recorded array data. The main idea was to improve the precision of such estimates by averaging over time (computing RMS values over an extended Lg window), frequency (using a bandpass filter covering all frequencies with significant Lg energy) and space (by averaging individual array elements). For a detailed description of the method and initial studies, reference is made to Ringdal and Hokland (1987); and Ringdal and Fyen (1988).

In this paper, we present some additional results from analysis of NORSAR and Gräfenberg Lg recordings of presumed underground explosions at the Shagan River area near Semipalatinsk, USSR. In particular, relative to earlier results, the Gräfenberg data base has been expanded to include all available recordings from these events. Furthermore, we have assessed the effects of introducing station corrections for individual array elements and epicentral distance corrections in the estimation procedure. The precision in the estimates has been investigated taking into account the signal-to-noise ratios, and a comparative analysis of NORSAR and Gräfenberg Lg measurements has been carried out.

Data sources

The NORSAR array (Bungum, Husebye and Ringdal, 1971) was established in 1970, and originally comprised 22 subarrays, deployed over an area of 100 km diameter. Since 1976 the number of operational subarrays has been 7, comprising altogether 42 vertical-component SP sensors (type HS-10). In this paper, analysis has been restricted to data from these 7 subarrays. Sampling rate for the NORSAR SP data is 20 samples per second, and all data are recorded on digital magnetic tape.

The Gräfenberg array (Harjes and Seidl, 1978) was established in 1976, and today comprises 13 broadband seismometer sites, three of which are 3-component systems. The instrument response is flat to velocity from about 20 second period to 5 Hz. Sampling rate is 20 samples per second, and the data are recorded on digital magnetic tape.

The location of NORSAR and Gräfenberg relative to Semipalatinsk is shown in Fig. VII.6.1, where also the propagation paths to the two arrays are indicated.

Based on ISC and NEIC reports, a total of 94 events, presumed to be nuclear explosions at the Shagan River area, have been selected as a data base. The time span is from 1965 to September 14, 1988, when the second Joint Verification Experiment (JVE) explosion was carried out. Table VII.6.1 lists the dates of these events together with pertinent measurements discussed later in the text.

Data analysis

All available recordings from NORSAR and GRF have been analyzed for the event set of 94 Shagan River explosions, using the procedure described by Ringdal and Hokland (1987).

Briefly, this procedure comprises filtering all array channels with a 0.6-3.0 Hz bandpass filter, computing RMS value of each filtered trace in a 2-minute Lg window (starting 12 min after P onset for NORSAR, 14 min for GRF), and compensating for background noise preceding P-onset. The Lg magnitude is then estimated by logarithmic averaging across each array.

The total number of available recordings with sufficient signal-to-noise ratio to allow reliable Lg measurement was 70 for NORSAR (starting in 1971) and 60 for GRF (starting in 1976).

While the NORSAR array configuration has been stable over the time period considered, the GRF array initially comprised only the four instruments A1 - A4, and was later expanded to its full configuration of 13 sites. In order to reduce as far as possible the bias due to changing array configurations, we have therefore computed station corrections for each individual GRF sensor (Table VII.6.2) and applied these in the array averaging procedure. A similar set of corrections for NORSAR are listed in Table VII.6.3. In practice, the introduction of station corrections has made little difference for the NORSAR magnitude estimates, but had a significant effect for GRF.

The effects of epicentral distance differences on the Lg magnitude estimates have also been assessed. The distance correction $B(\Delta)$ is determined through (Nuttli, 1986b):

$$B(\Delta) = [\sin(\Delta/111) \ / \ \sin(\Delta_0/111)]^{1/2} \cdot \exp[\gamma(\Delta-\Delta_0)]$$

Δ_0 is the distance (km) to a fixed reference location within the epicentral area (for Semipalatinsk we have used 50°N, 49°E) and Δ is the distance (km) to the event. γ is the coefficient of anelastic attenuation. We have used $\gamma = 0.001$ km^{-1}, which is near the value obtained by Nuttli (1986b) for 1 second Lg waves for paths from Semipalatinsk to Scandinavian stations. Note that a very accurate value of γ is not required when considering a limited source region, as the effects of small variations in this parameter on the resulting m_b(Lg) values are negligible.

The Lg magnitudes at NORSAR and GRF of events in the data base are listed in Table VII.6.1. Since these estimates take into account both station terms and epicentral distance corrections, they are slightly different from values published earlier, but nevertheless in good agreement.

Table VII.6.1 also contains estimated standard deviations of the Lg magnitudes, taking into account both the scattering across each array, the signal-to-noise ratios and the variance reduction obtained by the averaging procedure (see Appendix). We emphasize that these standard deviations are indicative only of the precision of measurement, and should not be interpreted as being representative of the accuracy of these magnitudes as source size estimators. We note that magnitudes of the larger explosions may be measured with very high precision, whereas the uncertainty is greater for the smaller events, due to the lower signal-to-noise ratios. It is also clear that the NORSAR-based estimates are more precise than those using GRF data, especially for events for which full GRF array recordings are not available.

Fig. VII.6.2 shows a scatter plot of NORSAR versus GRF magnitudes for all common events. The straight line represents a least squares fit to the data, assuming no errors in NORSAR magnitudes. We note that the two arrays show excellent consistency, although there is some increase in the scattering at low magnitudes. The standard deviation of the differences relative to the least squares fit is 0.045 magnitude units. Also there is no significant separation between events from NE and SW Shagan with regard to the relative Lg magnitudes observed at the two arrays.

In Fig. VII.6.3 a similar plot is shown, including only "well-recorded" events, i.e., requiring at least 5 operational GRF channels and a standard deviation of each array estimate not exceeding 0.04 magnitude units. The slope of the straight line fit has been restricted to the same value (1.15) as in Fig. VII.6.2. We note that there is a significant reduction in the scatter, and the standard deviation of the residuals is only 0.032 magnitude units. Thus the Lg magnitudes measured at the two arrays show excellent consistency for high signal-to-noise ratio events.

The slope (1.15) of the straight-line fit in Fig. VII.6.2 is slightly greater than 1.00, a tendency also noted by Ringdal and Fyen (1988): The interpretation of this observation is somewhat uncertain; a possible explanation is scaling differences in the Lg source spectrum (Kværna and Ringdal, 1988), in combination with the response differences of the NORSAR and GRF instruments. We have attempted to compare the two data sets after adjusting the GRF recordings to a NORSAR-type response. However, the results were inconclusive since the GRF signal-to-noise ratio then became too low for the smaller events.

Fig. VII.6.4 illustrates the pattern of P-Lg bias in the Shagan River area, using m_b values computed at Blacknest (Marshall, personal communication) together with combined NORSAR/GRF Lg magnitudes. The latter have been derived by adjusting the GRF magnitudes to an "equivalent" NORSAR value using the straight-line relation of Fig. VII.6.3, and then calculating a weighted average using the inverse variances (Table VII.6.1) as weighting factors. Fig. VII.6.4 includes all events of $m(Lg) \geq 5.6$, assuming either two-array observations or very precise Lg measurements from one array ($\sigma < 0.04$).

Although both the m_b values and the Lg magnitudes have been revised relative to those used in earlier studies, Fig. VII.6.4 confirms the observations previously made regarding the systematic difference between P-Lg residuals from NE and SW Shagan. In the NE area, $m_b(P)$ is generally lower than $m(Lg)$, whereas the opposite behavior is seen in the SW portion. The JVE explosion of 14 September 1988 has a P-Lg bias of 0.06 which is close to the average for the SW region. Furthermore, there appears to be a transition zone between the two portions of the test site, where the residuals are close to zero.

Conclusions

From this and previous studies, we can conclude that the Lg RMS estimation methods provide very stable, mutually consistent results when applied to two widely separated arrays (NORSAR and GRF). This is of clear significance regarding the potential use of such Lg measurements for yield estimation. Further research will be directed toward expanding the data base by conducting similar studies using other available station data as well as studying Lg recordings from other test sites. In particular, seismic data that might become available from USSR stations in the future would be of importance both in further assessing the stability of the estimates and to obtain Lg magnitudes for explosions of low yields.

F. Ringdal
J. Fyen

References

Baumgardt, D.R. (1985): Comparative analysis of teleseismic P coda and Lg waves from underground explosions in Eurasia. Bull. Seism. Soc. Amer., 75, 1413-1433.

Bungum, H., E.S. Husebye and F. Ringdal (1971): The NORSAR array and preliminary results of data analysis. Geophys. J., 25, 115-126.

Harjes, H.-P. and D. Seidl (1978): Digital recording and analysis of broadband seismic data at the Gräfenberg (GRF) array. J. Geophys. Res., 44, 511-523.

Kværna, T. and F. Ringdal (1988): Spectral analysis of Shagan River explosions recorded at NORSAR and NORESS (This volume).

Nuttli, O.W. (1973): Seismic wave attenuation and magnitude relations for eastern North America. J. Geophys. Res., 78, 876-885.

Nuttli, O.W. (1986a): Yield estimates of Nevada test site explosions obtained from seismic Lg waves. J. Geophys. Res., 91, 2137-2151.

Nuttli, O.W. (1986b): Lg magnitudes of selected East Kazakhstan underground explosions. Bull. Seism. Soc. Amer., 76, 1241-1251.

Ringdal, F. (1983): Magnitudes from P coda and Lg using NORSAR data. In: NORSAR Semiannual Tech. Summ., 1 Oct 1982 - 31 Mar 1983, NORSAR Sci. Rep. 2-82/83, Kjeller, Norway.

Ringdal, F. and B.Kr. Hokland (1987): Magnitudes of large Semipalatinsk explosions using P coda and Lg measurements at NORSAR. In: Semiannual Tech. Summ., 1 Apr - 30 Sep 1987, NORSAR Sci. Rep. 1-87/88, Kjeller, Norway.

Ringdal, F. and J. Fyen (1988): Analysis of Gräfenberg Lg recordings of Semipalatinsk explosion. In: Semiannual Tech. Summ., 1 Oct 1987 - 31 Mar 1988, NORSAR Sci. Rep. 2-87/88, Kjeller, Norway.

No.	ORIGIN DATE	ORIGIN TIME	MB	**** NORSAR **** M(LG)	N	STD ****	***** GRF ***** M(LG)	N	STD
1	01/15/65	5 59 58	5.8	-	-	-	-	-	-
2	06/19/68	5 05 57	5.4	-	-	-	-	-	-
3	11/30/69	3 32 57	6.0	-	-	-	-	-	-
4	06/30/71	3 56 57	5.2	-	-	-	-	-	-
5	02/10/72	5 02 57	5.4	-	-	-	-	-	-
6	11/02/72	1 26 57	6.1	6.116	42	0.014	-	-	-
7	12/10/72	4 27 7	6.0	6.115	42	0.009	-	-	-
8	07/23/73	1 22 57	6.1	6.195	40	0.006	-	-	-
9	12/14/73	7 46 57	5.8	5.866	42	0.033	-	-	-
10	04/16/74	5 52 57	4.9	-	-	-	-	-	-
11	05/31/74	3 26 57	5.9	-	-	-	-	-	-
12	10/16/74	6 32 57	5.5	5.409	42	0.024	-	-	-
13	12/27/74	5 46 56	5.6	5.711	42	0.056	-	-	-
14	04/27/75	5 36 57	5.6	5.547	42	0.057	-	-	-
15	06/30/75	3 26 57	5.0	-	-	-	-	-	-
16	10/29/75	4 46 57	5.8	5.628	42	0.046	-	-	-
17	12/25/75	5 16 57	5.7	5.794	42	0.035	-	-	-
18	04/21/76	5 2 57	5.3	-	-	-	-	-	-
19	06/09/76	3 2 57	5.3	5.200	42	0.089	-	-	-
20	07/04/76	2 56 57	5.8	5.811	42	0.009	5.785	4	0.024
21	08/28/76	2 56 57	5.8	5.734	41	0.013	5.654	3	0.052
22	11/23/76	5 02 57	5.8	-	-	-	5.794	3	0.057
23	12/07/76	4 56 57	5.9	-	-	-	5.702	3	0.088
24	05/29/77	2 56 57	5.8	5.673	41	0.035	5.570	3	0.038
25	06/29/77	3 6 58	5.3	5.031	40	0.110	-	-	-
26	09/05/77	3 2 57	5.8	5.893	40	0.017	5.768	3	0.036
27	10/29/77	3 7 2	5.6	5.788	41	0.043	5.685	3	0.041
28	11/30/77	4 06 57	6.0	-	-	-	5.716	3	0.041
29	06/11/78	2 56 57	5.9	5.750	39	0.029	5.724	4	0.039
30	07/05/78	2 46 57	5.8	5.795	39	0.010	-	-	-
31	08/29/78	2 37 6	5.9	6.009	39	0.008	6.001	6	0.022
32	09/15/78	2 36 57	6.0	5.908	38	0.018	-	-	-
33	11/04/78	5 5 57	5.6	5.672	39	0.088	5.624	6	0.080
34	11/29/78	4 33 2	6.0	5.969	39	0.013	5.828	2	0.075
35	02/01/79	4 12 57	5.4	-	-	-	-	-	-
36	06/23/79	2 56 57	6.2	6.056	21	0.009	6.113	4	0.021
37	07/07/79	3 46 57	5.8	5.968	38	0.008	5.940	7	0.021
38	08/04/79	3 56 57	6.1	6.101	39	0.008	6.106	9	0.015
39	08/18/79	2 51 57	6.1	-	-	-	6.138	7	0.017
40	10/28/79	3 16 56	6.0	6.054	34	0.010	6.050	8	0.023
41	12/02/79	4 36 57	6.0	5.916	28	0.021	5.949	10	0.025
42	12/23/79	4 56 57	6.2	-	-	-	6.042	9	0.021
43	04/25/80	3 56 57	5.5	-	-	-	-	-	-
44	06/12/80	3 26 57	5.6	-	-	-	5.575	11	0.105
45	06/29/80	2 32 57	5.7	5.680	16	0.026	5.744	8	0.046
46	09/14/80	2 42 39	6.2	-	-	-	-	-	-
47	10/12/80	3 34 14	5.9	5.927	28	0.013	5.938	13	0.034
48	12/14/80	3 47 6	5.9	5.931	28	0.018	5.948	10	0.027
49	12/27/80	4 9 8	5.9	5.936	27	0.014	5.886	11	0.034
50	03/29/81	4 3 50	5.6	5.555	28	0.085	5.439	11	0.184

Table VII.6.1. List of presumed explosions at the Shagan River test area near Semipalatinsk, USSR. The m_b values are those published in the ISC bulletins for events prior to 1986, and are otherwise taken from NEIC/PDE reports. NORSAR and Gräfenberg Lg RMS magnitudes are given for all events with available recordings of sufficient signal-to-noise ratio. The number of data channels used and the estimated precision of measurements (see Appendix) are given for each magnitude value. (Page 1 of 2).

No.	ORIGIN DATE	ORIGIN TIME			MB	**** NORSAR **** M(LG)	N	STD	***** GRF ***** M(LG)	N	STD
51	04/22/81	1	17	11	6.0	5.907	28	0.022	5.956	11	0.027
52	05/27/81	3	58	12	5.5	5.456	27	0.023	-	-	-
53	09/13/81	2	17	18	6.1	6.114	29	0.008	6.109	9	0.015
54	10/18/81	3	57	2	6.1	5.984	34	0.010	5.956	9	0.021
55	11/29/81	3	35	8	5.7	5.545	28	0.121	5.512	12	0.192
56	12/27/81	3	43	14	6.2	6.071	34	0.009	6.050	9	0.021
57	04/25/82	3	23	5	6.1	6.078	35	0.008	6.069	10	0.017
58	07/04/82	1	17	14	6.1	-	-	-	-	-	-
59	08/31/82	1	31	0	5.3	-	-	-	-	-	-
60	12/05/82	3	37	12	6.1	5.988	31	0.019	6.001	13	0.020
61	12/26/82	3	35	14	5.7	5.655	39	0.080	5.598	13	0.067
62	06/12/83	2	36	43	6.1	6.073	25	0.009	-	-	-
63	10/06/83	1	47	6	6.0	5.867	19	0.033	5.851	11	0.040
64	10/26/83	1	55	4	6.1	5.999	33	0.021	6.035	11	0.020
65	11/20/83	3	27	4	5.5	-	-	-	-	-	-
66	02/19/84	3	57	3	5.9	5.723	29	0.038	-	-	-
67	03/07/84	2	39	6	5.7	5.695	29	0.065	5.575	12	0.108
68	03/29/84	5	19	8	5.9	5.899	29	0.012	5.961	13	0.043
69	04/25/84	1	9	3	6.0	5.869	35	0.008	5.804	13	0.031
70	05/26/84	3	13	12	6.0	6.073	33	0.007	6.132	13	0.015
71	07/14/84	1	9	10	6.2	6.055	32	0.007	6.066	12	0.015
72	09/15/84	6	15	10	4.7	-	-	-	-	-	-
73	10/27/84	1	50	10	6.2	6.082	33	0.011	6.143	13	0.016
74	12/02/84	3	19	6	5.8	5.881	29	0.020	5.864	12	0.036
75	12/16/84	3	55	2	6.1	6.046	29	0.010	6.037	13	0.014
76	12/28/84	3	50	10	6.0	5.982	35	0.009	5.944	13	0.021
77	02/10/85	3	27	7	5.9	5.801	40	0.024	5.800	13	0.058
78	04/25/85	0	57	6	5.9	5.859	29	0.045	5.848	7	0.047
79	06/15/85	0	57	0	6.0	5.976	30	0.009	6.031	13	0.017
80	06/30/85	2	39	2	6.0	5.928	30	0.009	5.905	12	0.018
81	07/20/85	0	53	14	5.9	5.858	37	0.013	5.867	12	0.031
82	03/12/87	1	57	17	5.5	5.215	33	0.076	-	-	-
83	04/03/87	1	17	8	6.2	6.051	33	0.008	6.126	11	0.017
84	04/17/87	1	3	4	6.0	5.898	33	0.020	5.912	12	0.026
85	06/20/87	0	53	4	6.1	5.968	36	0.007	5.943	10	0.028
86	08/02/87	0	58	6	5.9	-	-	-	5.856	11	0.022
87	11/15/87	3	31	6	6.0	5.973	37	0.008	5.983	13	0.022
88	12/13/87	3	21	4	6.1	6.091	31	0.010	6.066	12	0.015
89	12/27/87	3	5	4	6.1	6.046	31	0.011	6.032	13	0.019
90	02/13/88	3	5	5	6.1	6.042	26	0.009	6.047	13	0.029
91	04/03/88	1	33	5	6.1	6.067	31	0.007	6.076	13	0.014
92	05/04/88	0	57	6	6.1	6.040	31	0.008	6.064	13	0.020
93	06/14/88	2	27	6	4.9	-	-	-	-	-	-
94	09/14/88	4	0	0	6.0	5.969	37	0.010	5.970	12	0.043

Table VII.6.1. (Page 2 of 2)

CHANNEL NO	BIAS	N	STD
1	0.15	24	0.029
2	0.15	31	0.031
3	0.19	24	0.042
4	0.08	19	0.034
5	0.01	12	0.046
6	-0.11	18	0.030
7	0.01	16	0.041
8	0.09	15	0.036
9	-0.09	19	0.039
10	-0.15	13	0.024
11	-0.04	7	0.033
12	-0.17	12	0.039
13	-0.12	14	0.045

<u>Table VII.6.2.</u> List of station terms (station RMS Lg value minus array average) for the Gräfenberg array. The 13 individual vertical component seismometers are listed in the sequence A1-4, B1-5 and C1-4. The bias values are based on high signal-to-noise ratio events recorded by at least 10 channels. The number of observations and the sample standard deviation is listed for each instrument.

CHANNEL NO	BIAS	N	STD
1	0.05	49	0.051
2	0.11	31	0.044
3	0.17	23	0.044
4	0.04	6	0.025
5	0.10	45	0.028
6	-0.01	49	0.060
7	0.01	43	0.033
8	0.08	39	0.045
9	-0.01	42	0.029
10	0.13	42	0.036
11	0.00	34	0.047
12	0.05	43	0.042
13	0.03	48	0.038
14	-0.11	48	0.028
15	-0.01	49	0.033
16	-0.01	49	0.035
17	0.03	49	0.032
18	-0.02	49	0.040
19	-0.02	43	0.033
20	-0.01	44	0.043
21	-0.05	45	0.034
22	-0.05	45	0.024
23	-0.03	44	0.049
24	-0.04	46	0.022
25	-0.10	45	0.031
26	0.02	45	0.037
27	-0.07	44	0.027
28	-0.08	45	0.023
29	-0.02	45	0.031
30	-0.02	45	0.038
31	-0.06	42	0.031
32	-0.01	42	0.025
33	-0.03	41	0.047
34	-0.02	43	0.033
35	-0.04	44	0.029
36	0.01	40	0.055
37	-0.04	21	0.031
38	-0.05	32	0.030
39	0.01	20	0.064
40	-0.01	19	0.046
41	0.02	18	0.036
42	0.05	20	0.029

Table VII.6.3. List of station terms (station RMS Lg value minus array average) for the NORSAR array. The 42 individual seismometers are listed in the standard sequence (subarrays 01A through 06C). The bias values are based on events with high signal-to-noise ratio (Lg magnitude > 5.8). The number of observations and the sample standard deviation are listed for each instrument.

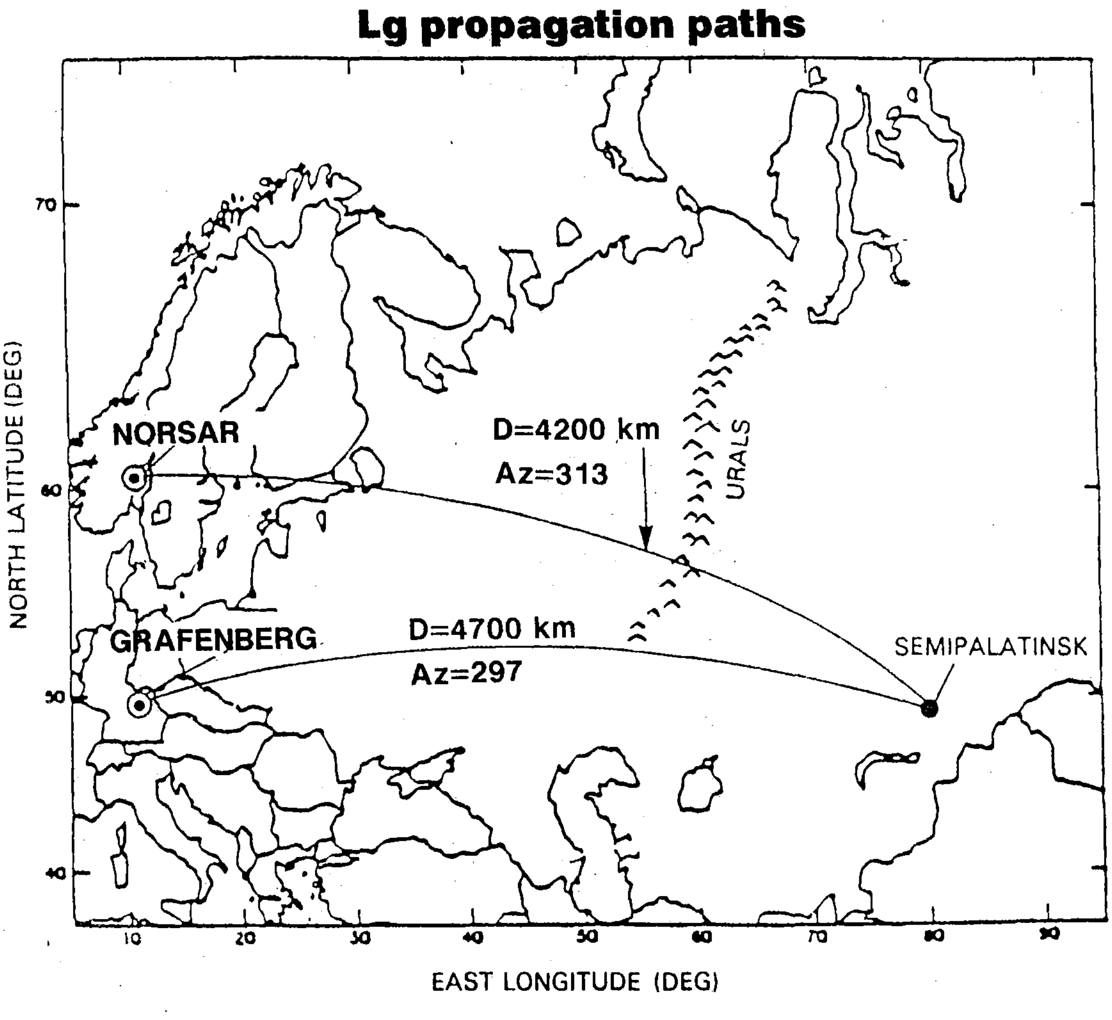

Fig. VII.6.1. Location of the NORSAR and Gräfenberg arrays in relation to the Semipalatinsk test site.

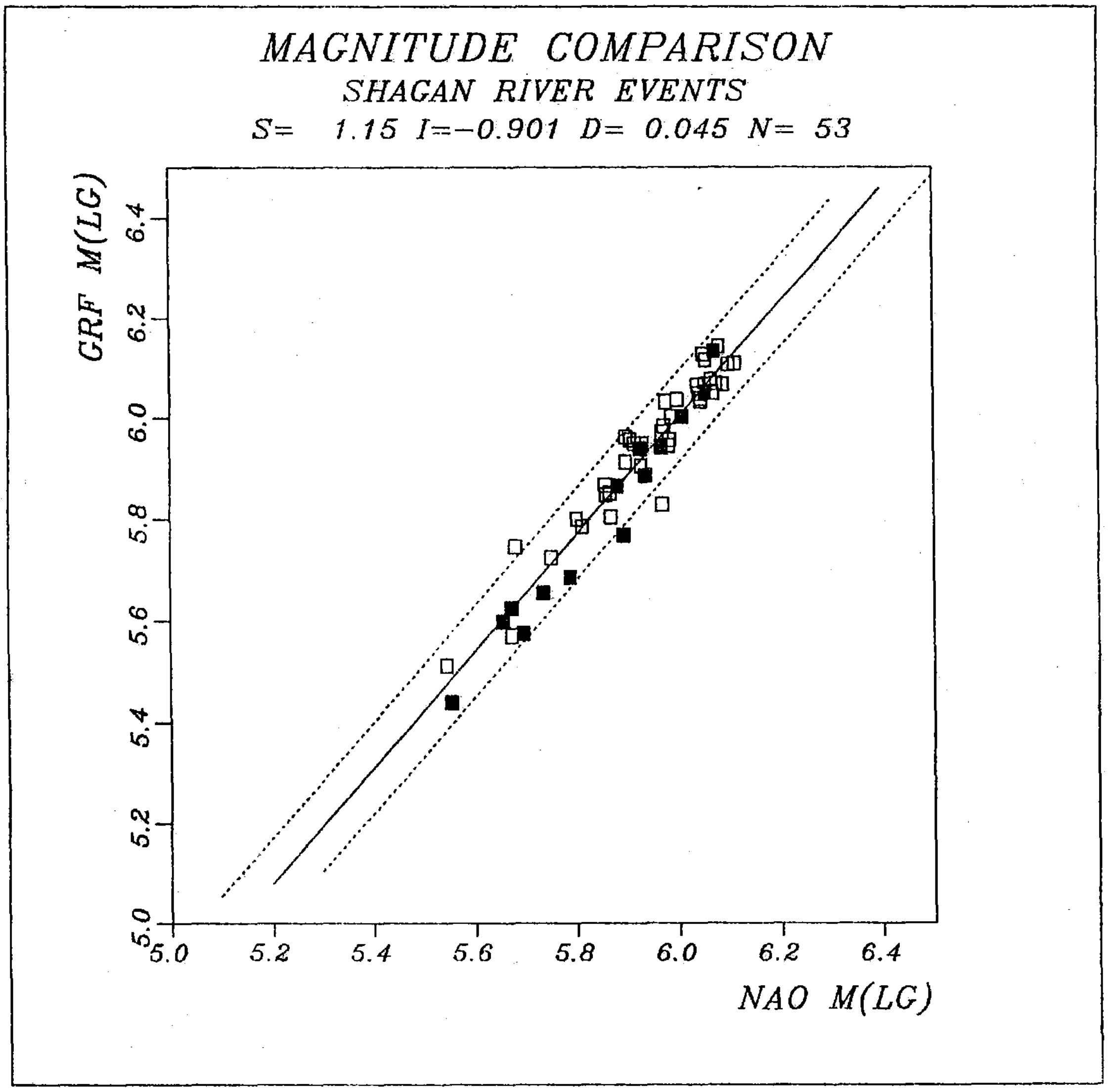

Fig. VII.6.2. Plot of Gräfenberg (GRF) versus NORSAR (NAO) Lg magnitudes for Shagan River explosions. The figure includes all common events in Table VII.6.1. Events in the NE and SW parts of Shagan are marked as filled squares and open squares, respectively. The straight line (slope 1.15) represents a least squares fit to the data, assuming no error in NORSAR Lg measurements. The standard deviation of the residuals along the vertical axis relative to the straight line is 0.045, and the dotted lines correspond to plus/minus two standard deviations.

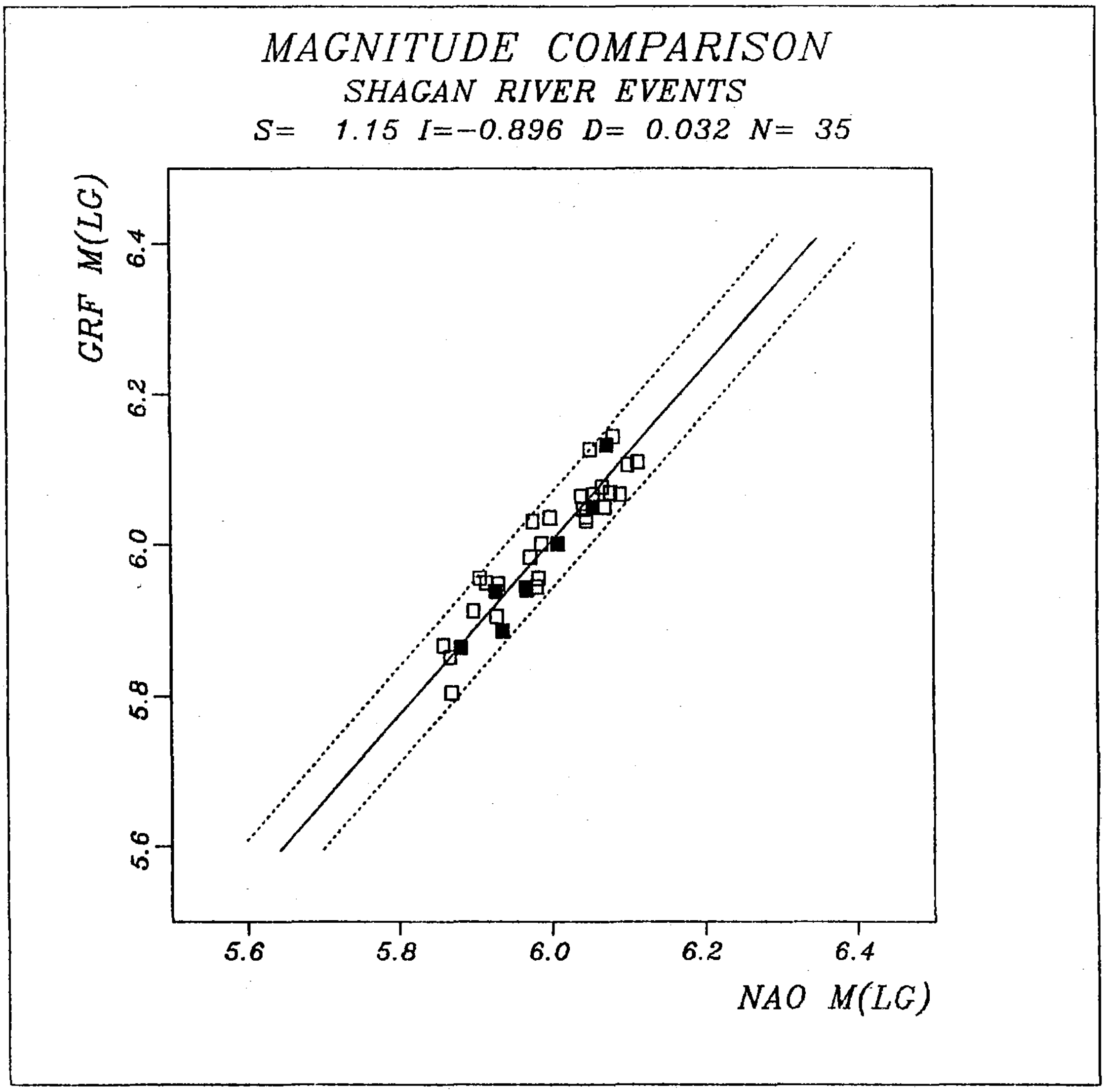

Fig. VII.6.3. Same as Fig. VII.6.2, but showing only "well-recorded" events, i.e., requiring at least 5 operational GRF channels and a standard deviation of each array estimate not exceeding 0.04. The slope of the straight line has been restricted to the value obtained in Fig. VII.6.2. Note that the scatter in the data has been significantly reduced, and the standard deviation in the vertical direction is only 0.032 magnitude units for this data set.

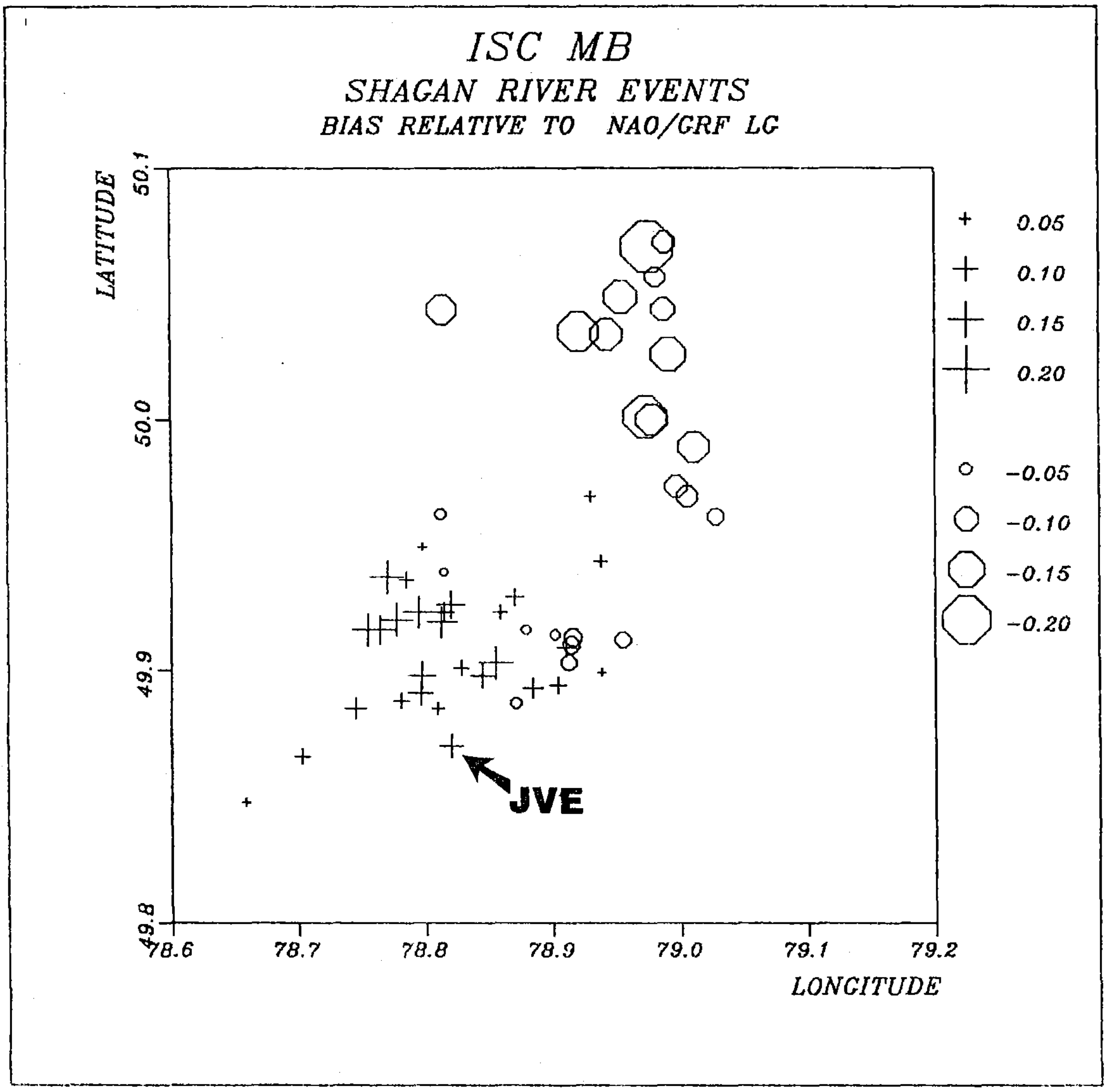

Fig. VII.6.4. Plot of P-Lg magnitude residuals (ISC maximum likelihood minus NORSAR/Gräfenberg Lg magnitudes) as a function of event location (Marshall, personal communication) within the Shagan River area. Plusses and circles correspond to residuals greater or less than the average, respectively, with symbol size proportional to the deviation. All events of $m_b(Lg) \geq 5.6$ for which we have precise locations have been included, assuming either two-array observations or very precise Lg measurements from one array. The JVE explosion is especially marked. Note the systematic variation from NE to SW Shagan, with an apparent transition zone in between.

Appendix to Section VII.6

In this appendix we develop an approximate expression for the uncertainty in the RMS Lg magnitude estimates described earlier. We first consider the case of a single sensor measurement, and afterwards address the array averaging procedure.

Denote by $x_1(t)$ the recorded signal in the "Lg window", and assume that this is composed of a noise component $x_2(t)$ and a signal component $x_3(t)$ as follows:

$$x_1(t) = x_2(t) + x_3(t) \qquad (1)$$

Here, we assume that the noise component $x_2(t)$ can be modelled as a zero-mean random process which is stationary over a time interval long enough to include both the Lg window and a suitable noise window preceding the P onset. The signal $x_3(t)$ is considered a zero-mean random process defined in the Lg time window, and being uncorrelated with $x_2(t)$.

We can thus obtain an estimate of the mean square value X_3 of $x_3(t)$ by

$$X_3 = X_1 - X_2 \qquad (2)$$

where X_1 is the mean square value of $x_1(t)$ in the signal window, and X_2 is the mean square value of $x_2(t)$ in the noise window.

The Lg RMS magnitude is then (apart from an additive constant) determined as $\log_{10} \sqrt{X_3}$.

We now make the assumption that the quantities X_i $(i=1,\ldots,3)$ each follow a lognormal distribution, when considered as random variables. We emphasize that this assumption, which is reasonable in view of empirical studies of logarithmic amplitude patterns of signals and noise, represents an approximation only. Thus, we know that the difference between two lognormal variables is usually not another lognormal variable, but for our purposes this approximation is useful.

We may thus write (using natural logarithms):

$$\log X_i \text{ is } N(m_i,\ 4\sigma_i^2) \qquad i = 1,\ldots,3 \tag{3}$$

Note that using $4\sigma_i^2$ as the variance of $\log X_i$ corresponds to σ_i^2 representing the variance of the log RMS estimate.

The mean and variances of the respective variables can then be expressed by (Aitchison and Brown, 1969):

$$EX_i = e^{m_i+2\sigma_i^2} \qquad i = 1,\ldots,3 \tag{4}$$

$$\text{var } X_i = (EX_i)^2 \cdot (e^{4\sigma_i^2} - 1) \qquad i = 1,\ldots,3 \tag{5}$$

From eq. (2) we furthermore obtain

$$EX_3 = EX_1 - EX_2 \tag{6}$$

$$\text{var } X_3 = \text{var } X_1 + \text{var } X_2 \tag{7}$$

Combining (5) and (7), this leads to the relation:

$$(EX_2 - EX_1)^2 \cdot (e^{4\sigma_3^2} - 1) = (EX_1)^2 \cdot (e^{4\sigma_1^2} - 1) + (EX_2)^2 \cdot (e^{4\sigma_2^2} - 1) \tag{8}$$

Substituting EX_1 and EX_2 by the observed values $\hat{X}_1$ and $\hat{X}_2$, respectively, and assuming small values of σ_i ($i = 1,\ldots,3$) we obtain from (8) the following simplified relation:

$$\sigma_3^2 = \frac{\sigma_1^2 \cdot \hat{X}_1^2 + \sigma_2^2 \cdot \hat{X}_2^2}{(\hat{X}_1 - \hat{X}_2)^2} \tag{9}$$

which represents an approximate expression for the variance of $\log\sqrt{X_3}$. Note that (9) is developed using natural logarithms, it applies without change if base 10 logarithms are used throughout.

Although we have used a number of simplifications in arriving at (9), simulation experiments using randomly generated distributions have shown that this formula gives a useful approximation to the actual scatter in the estimates within a reasonable range of parameter values.

We note that in cases of high signal-to-noise ratios, (i.e., $\hat{X}_1 >> \hat{X}_2$), we obtain from (9) $\sigma_3^2 \approx \sigma_1^2$; thus the noise variance has no significant effect on the Lg magnitude variance. On the other hand, as the signal-to-noise ratio becomes small, the variance σ_3^2 will increase rapidly.

In the array averaging procedure, we assume that the term σ_1^2 is reduced in proportion to the number of array elements, whereas we consider σ_2^2 to represent mainly a systematic noise fluctuation that is not reduced through array averaging.

Defining the signal-to-noise ratio α by $\alpha = \hat{X}_1/\hat{X}_2$, and denoting by N the number of array elements, we thus obtain from (9)

$$\sigma_3^2 = \frac{(\sigma_1^2 \cdot \alpha^2)/N + \sigma_2^2}{(\alpha - 1)^2} \tag{10}$$

As a numerical example, consider the JVE explosion (event 94 in Table VII.6.1).

For NORSAR, we have estimated $\alpha = 13.12$, with $N = 37$, and we assume $\sigma_1 = 0.04$, $\sigma_2 = 0.08$. Formula (10) then gives $\sigma_3 = 0.010$.

For GRF, we have $\alpha = 3.03$, with $N = 12$, and the same input σ values as above then give $\sigma_3 = 0.043$. Thus, the estimated uncertainty of the GRF Lg magnitude is considerably greater than that of NORSAR, the main reason being the lower signal-to-noise ratio for GRF.

Reference

Aitchison, J. and J.A.C. Brown (1969): The Lognormal Distribution, Cambridge University Press, UK.